FULL PAPER

Standardizing Monte Carlo simulation parameters for a reproducible dose-averaged linear energy transfer

[1]WEI YANG CALVIN KOH, [2]HONG QI TAN, [2]KHONG WEI ANG, [2]SUNG YONG PARK, [1]WEN SIANG LEW and
[1,2]JAMES CHEOW LEI LEE

[1]Division of Physics and Applied Physics, Nanyang Technological University, Singapore, Singapore
[2]Division of Radiation Oncology, National Cancer Centre Singapore, Singapore, Singapore

Address correspondence to: Mr Wei Yang Calvin Koh
E-mail: *calvin.kohwy@gmail.com*

Objective: Dose-averaged linear energy transfer (LET_D) is one of the factors which determines relative biological effectiveness (RBE) for treatment planning in proton therapy. It is usually determined from Monte Carlo (MC) simulation. However, no standard simulation protocols were established for sampling of LET_D. Simulation parameters like maximum step length and range cut will affect secondary electrons production and have an impact on the accuracy of dose distribution and LET_D. We aim to show how different combinations of step length and range cut in GEANT4 will affect the result in sampling of LET_D using different MC scoring methods.
Methods: In this work, different step length and range cut value in a clinically relevant voxel geometry were used for comparison. Different LET_D scoring methods were established and the concept of covariance between energy deposition per step and step length is used to explain the differences between them.

Results: We recommend a maximum step length of 0.05 mm and a range cut of 0.01 mm in MC simulation as this yields the most consistent LET_D value across different scoring methods. Different LET_D scoring methods are also compared and variation up to 200% can be observed at the plateau of 80 MeV proton beam. Scoring *Method one* has one of the lowest percentage differences compared across all simulation parameters.
Conclusion: We have determined a set of maximum step length and range cut parameters to be used for LET_D scoring in a 1 mm voxelized geometry. LET_D scoring method should also be clearly defined and standardized to facilitate cross-institutional studies.
Advances in knowledge: Establishing a standard simulation protocol for sampling LET_D would reduce the discrepancy when comparing data across different centres, and this can improve the calculation for RBE.

INTRODUCTION

In radiation therapy, dose is used an indicator for inducing cell death and thus tumour control. However, in proton therapy, LET_D is one of the independent variables required for the calculation of *relative biological effectiveness* (RBE)[1–3]. In fact, McMahon *et al*[1] had reported that there is a better correlation between cell survival curve and both *dose* and *dose-averaged linear energy transfer* (LET_D) as compared to solely *dose* in proton irradiation. This further exemplifies that LET_D affects the biological effective dose calculation and it should be determined meticulously.

LET values are difficult to measure experimentally[4,5] and thus they are often determined analytically[6] or via simulation[7,8]. Monte Carlo (MC) simulation is usually used for this purpose as it is regarded as the gold standard in radiation transport simulation[9]. Although MC simulation is used extensively in various applications (Medical, Space

and Radiation Protection), the results depend heavily on the physics models and the parameters incorporated in the simulation.

Despite the known importance of LET values and its effect on cell killing[10,11], there is still a lack of studies investigating the credibility of the methods to obtain LET values from MC simulation. The reproducibility of LET values will depend on the definition of LET: (a) track-averaged LET (LET_t) and (b) dose-averaged LET (LET_D) as represented by analytical equations discussed in Wilkens and Oelfke[6]. Furthermore, in MC simulation, parameters such as the choice of physics model, maximum step length (upper limit of a particle's tracking step length), range cut limits (minimum energy of secondary particles in inelastic interaction) and voxel dimensions can also cause a variation in the scoring of LET. Since LET_D is used for the calculation of

RBE[1–3], it will be the main focus in this work and the analytical equation is calculated using

$$LET_D\left(\vec{r}\right) = \frac{\int D\left(E, \vec{r}\right) LET\left(E\right) dE}{\int D\left(E, \vec{r}\right) dE} \qquad (1)$$

where $D\left(E, \vec{r}\right)$ is the dose deposited by the proton with energy E at location $\vec{r}$[12]. However, in MC simulation, LET$_D$ is generally expressed as

$$LET_D = \frac{\sum_{i=1}^{n} \frac{\epsilon_i^2}{l_i}}{\sum_{i=1}^{n} \epsilon_i} \qquad (2)$$

where ϵ_i is the energy deposition by the ith charged particle, l_i is the step length and n is the total number of steps in the each voxel[4,5,13]. As defined in ICRU Report No. 85[14], LET is the *average energy transfer* by the charged particle per unit length due to electronic interactions at a spatial point. This definition of LET is limited to one specified type of charged particles (proton, electron and other heavy ion) at any one point of time. However, LET$_D$ is used in this work as it accounts for an ensemble of charged particles in a particular voxel instead of considering only one type of particle and this has higher correlation to biological damage. Since primary protons and secondary electrons both contribute to the biological damage in real-life situation, they should be included in LET$_D$ calculation. Therefore, the LET$_D$ is simplified to the *total energy deposited* by the charged particles in MC simulation[4] as described by **Eq**. (2).

There were several works done on using MC simulation to sample LET$_D$. A large range cut for secondary electrons is often used in a typical MC simulation for proton therapy application[15,16] because of the increased computation time for explicit electron tracking. This poses a problem in a real-life situation of a lung patient where the electrons do travel over a higher range due to the low density of lung and secondary electrons need to be factored in for greater dose accuracy. As demonstrated by Guan *et al*[4], they used GEANT4 MC toolkit[17–19] to simulate a proton beam with a high range cut (no explicit secondary electron production) and consider only electronic inelastic interactions (nuclear interactions are neglected) to compare LET$_D$ and LET$_t$ values. In the work by Cortes-Giraldo *et al*[20], they showed that there is a difference in the calculated LET$_D$ based on the

different LET$_D$ scoring methods, range cut and voxel dimensions used. However, their work was done using MC simulation with a cylindrical volume rather than a voxelized geometry which is used clinically.

In addition to the variation of parameters in MC simulation, the scoring methods for LET$_D$ differ with different studies. Both Guan *et al*[4] analysis of LET$_D$ and Granville *et al*[5] comparison of LET$_D$ scoring techniques use **Eq**. (2) for their LET$_D$ calculations. Similarly, Cortes-Giraldo *et al*[20] also used similar equations to **Eq**. (3), except that they had included a weighting factor to each equation to account for only primary protons in their LET$_D$ calculation. They had recommended a scoring method which provided a stable unrestricted LET$_D$ with different voxel sizes and production cuts. However, this method simplifies the LET$_D$ scoring method to unrestricted LET$_D$ and is similar to the *Unrestricted* method in **Sec**. (2). Thus, their method is excluded in our comparison. This shows that LET$_D$ scoring method is not clearly defined in MC and there is no strong physical basis on which scoring methods should be used in scoring LET$_D$ especially when both primary protons and secondary electrons are present in the simulation.

$$LET_D = \frac{\frac{\left(\sum_{i=1}^{n} \epsilon_i\right)^2}{\sum_{i=1}^{n} l_i}}{\sum_{i=1}^{n} \epsilon_i} \qquad (3)$$

In this work, we are interested in the scoring of both primary protons and secondary electrons due to the aforementioned problem in real-life situation. We examine the best step length (*stepMax*), range cut (*setCut*) value and LET$_D$ scoring methods (Table 1) that should be implemented in MC simulation to achieve a reproducible LET$_D$ value in a clinically relevant voxel geometry. Although LET$_D$ must be insensitive to variations of hyperparameters of the simulation, one should not omit the fact that hyperparameters do affect the LET$_D$ results. Therefore, we aim to propose and standardize a step length, range cut and LET$_D$ scoring method for MC simulation so as to obtain a most reproducible LET$_D$ result.
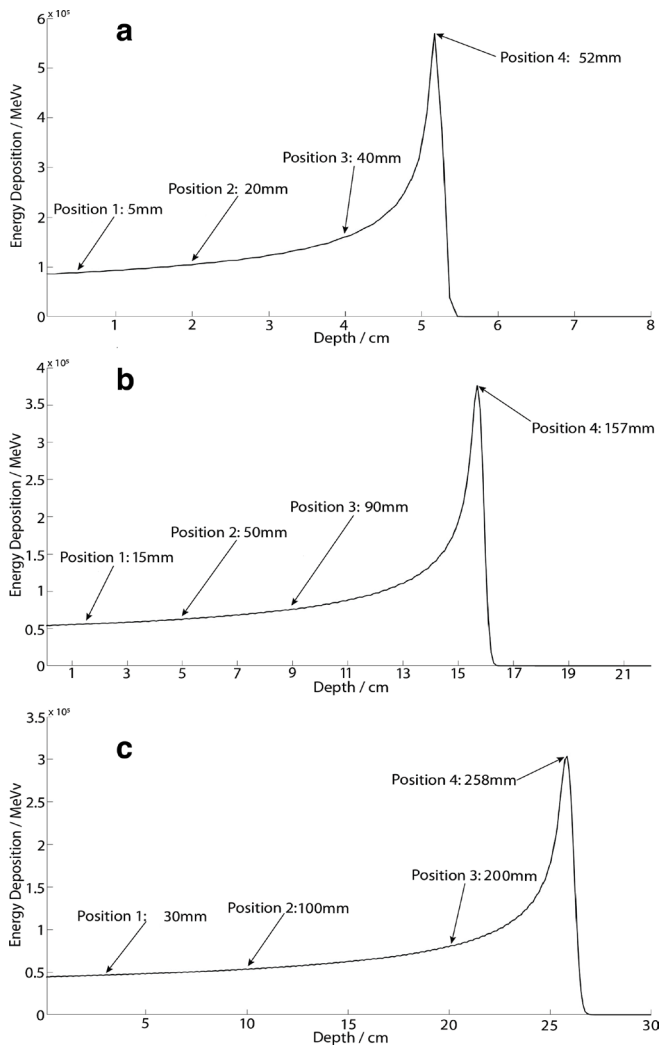
METHODS AND MATERIALS
MC simulation settings
A mono-energetic proton beam of 80 MeV, 150 MeV and 200 MeV were irradiated at central axis of a $30\times30\times30$ cm^3 water

Table 1. This table shows the *LET$_D$* scoring methods where $n_p\left(n_e\right)$ refers to the number of protons (electrons), $\epsilon_p\left(\epsilon_e\right)$ is the energy deposition of protons (electrons) and $l_p\left(l_e\right)$ is the step length of protons (electrons). The last row shows the mathematical expectation form of each corresponding *LET$_D$* scoring methods where $i \in p, e$.

Unrestricted	Method 1	Method 2	Method 3	Method 4
$\dfrac{\sum_{p=1}^{n_p} \frac{\epsilon_p^2}{l_p}}{\sum_{p=1}^{n_p} \epsilon_p}$	$\dfrac{\sum_{p=1}^{n_p} \frac{\epsilon_p^2}{l_p} + \sum_{e=1}^{n_e} \frac{\epsilon_e^2}{l_e}}{\sum_{p,e=1}^{n_p,n_e} \epsilon_p + \epsilon_e}$	$\dfrac{\frac{\sum_{p,e=1}^{n_p,n_e} \epsilon_p^2 + \epsilon_e^2}{\sum_{p,e=1}^{n_p,n_e} l_p + l_e}}{\frac{\sum_{p,e=1}^{n_p,n_e} \epsilon_p + \epsilon_e}{n_p + n_e}}$	$\dfrac{\frac{\sum_{p=1}^{n_p} \epsilon_p^2}{\sum_{p=1}^{n_p} l_p} + \frac{\sum_{e=1}^{n_e} \epsilon_e^2}{\sum_{e=1}^{n_e} l_e}}{\frac{\sum_{p,e=1}^{n_p,n_e} \epsilon_p + \epsilon_e}{n_p + n_e}}$	$\dfrac{\frac{\left(\sum_{p=1}^{n_p} \epsilon_p\right)^2}{\sum_{p=1}^{n_p} l_p} + \frac{\left(\sum_{e=1}^{n_e} \epsilon_e\right)^2}{\sum_{e=1}^{n_e} l_e}}{\sum_{p,e=1}^{n_p,n_e} \epsilon_p + \epsilon_e}$
$\dfrac{\mathrm{E}\left(\frac{\epsilon_p^2}{l_p}\right)}{\mathrm{E}\left(\epsilon_p\right)}$	$\dfrac{\mathrm{E}\left(\frac{\epsilon_i^2}{l_i}\right)}{\mathrm{E}\left(\epsilon_i\right)}$	$\dfrac{\frac{\mathrm{E}\left(\epsilon_i^2\right)}{\mathrm{E}\left(l_i\right)}}{\mathrm{E}\left(\epsilon_i\right)}$	$\dfrac{\frac{\mathrm{E}\left(\epsilon_p^2\right)}{\mathrm{E}\left(l_p\right)} + \frac{\mathrm{E}\left(\epsilon_e^2\right)}{\mathrm{E}\left(l_e\right)}}{\mathrm{E}\left(\epsilon_i\right)}$	$\dfrac{\frac{\left[\mathrm{E}\left(\epsilon_p\right)\right]^2}{\mathrm{E}\left(l_p\right)} + \frac{\left[\mathrm{E}\left(\epsilon_e\right)\right]^2}{\mathrm{E}\left(l_e\right)}}{\mathrm{E}\left(\epsilon_i\right)}$

Figure 1. (a) (b) and (c) show the Bragg peak of 80 MeV, 150 MeV and 200 MeV, respectively. Energy deposition and step length are scored individually for every particle in the selected voxels at Positions 1, 2, 3 and 4 of each proton beam energy.

Table 2. This table shows the MC simulation parameters of 3 proton beam energies, three step length and four range cut that are used in this work. *Unrestricted* refers to range cut of 10^6 mm.

Energy/MeV	stepMax/mm	setCut/mm
80	0.01	0.01
150	0.05	0.05
200	0.5	0.1
		Unrestricted: 10^6

Correlation between LET$_D$ scoring methods

In this work, we used the concept of correlation to understand differences between LET$_D$ scoring methods. Most of the differences in LET definition arises from the inequality of $E\left(\frac{\epsilon_i^2}{l}\right)$ and $\frac{E\left(\epsilon_i^2\right)}{E(l)}$. $E\left(\frac{\epsilon_i^2}{l}\right)$ can be approximated by **Eq**. (6)[21,22] from doing a bivariate second-order Taylor expansion. The first-order Taylor expansion was done at an expansion point $(\theta = \mu_x, \mu_y)$ where μ represents the mean of the variable. We will arrive at Eq. (4).

$$E\left(f\left(X,Y\right)\right) \approx f\left(E\left(X\right), E\left(Y\right)\right) = f\left(\mu_x, \mu_y\right) \qquad (4)$$

By doing the second-order Taylor expansion at the same expansion point θ, we can simplify to Eq. (5).

$$E(f(X,Y)) \approx f(\theta) + \frac{1}{2}(f_{xx}''(\theta)Var(X) + 2f_{xy}''(\theta)Cov(X,Y) + f_{yy}''(\theta)Var(Y)) \qquad (5)$$

Since we know that $\theta = \left(\mu_x, \mu_y\right)$, $f(\theta) = \frac{\mu_x}{\mu_y}$, $f_{xx}''\left(\theta\right) = 0$, $f_{xy}''\left(\theta\right) = -\frac{1}{\left(\mu_y\right)^2}$ and $f_{yy}''\left(\theta\right) = \frac{2\mu_x}{\left(\mu_y\right)^3}$, by substituting (x,y) with $\left(\epsilon_i^2, l_i\right)$, we will arrive at Eq. (6).

$$E\left(\frac{\epsilon_i^2}{l}\right) \approx \frac{E\left(\epsilon_i^2\right)}{E(l)} - \frac{Cov\left(\epsilon_i^2, l\right)}{\left(E(l)\right)^2} + \frac{Var(l)E\left(\epsilon_i^2\right)}{\left(E(l)\right)^3} \qquad (6)$$

It can be seen that the difference depends on the covariance of energy deposition and step length. Hence, if the distribution of ϵ^2 against l for all steps in a voxel is linearly correlated, it implies that the covariance will be high and the values of the LET$_D$ will be affected significantly by the definition.

Evaluation of LET$_D$ scoring methods in different simulation parameters

There are different ways to calculate the average LET in an ensemble of ϵ_p and l$_p$ (ϵ_e and l_e) pair. Table 1 shows the five different LET$_D$ scoring method to calculate LET$_D$ for each voxel and its respective mathematical expectation form. The LET$_D$ scoring methods are the possible ways to calculate LET$_D$ in MC simulation and the mathematical expectation form can be calculated from the relation in **Eq**. (7). The expectation is taken across all steps and events in the simulation and is defined similarly for all five methods. *Methods 1* to *4* include secondary electrons in

phantom using GEANT4 MC Toolkit, respectively. The water phantom is voxelized into $1\,mm^3$ cube and the z-coordinate (depth) of the water phantom ranges from 0 to 300 mm. The number of particle histories is set to 100,000 and the dose errors are less than 2% across the central axis of the dose. G4EmStandardPhysics_option 4 is used for physics model as it is the recommended physical model for clinical proton beam below 5 GeV[4].

Energy deposition and step length are scored individually for every particle in the selected voxels at *Positions 1, 2, 3* and *4* for each proton beam energy as shown in Figure 1 **a**, **b** and **c**. Positions beyond the Bragg peak were not chosen due to the absence of secondary electrons. There is no difference in the LET$_D$ calculated by the five scoring methods as most of the energies of the secondary electrons are below the range cut value, thus all calculation converges. The positions are described by the depth from the water phantom range as mentioned above. LET$_D$ is calculated from these parameters as shown in Table 2.

Figure 2. This figure shows LET$_D$ vs Depth for 80 MeV (top) and 200 MeV (bottom) proton beam with step length of 0.5 mm and a comparison of Unrestricted and 0.1 mm range cut. The additional plot focuses on the plateau region of the main graph. The ○ represents LET$_D$ values for Unrestricted setCut, Δ and □ represent LET$_D$ values for 0.1 mm range cut, considering only protons and protons + secondary electrons, respectively.
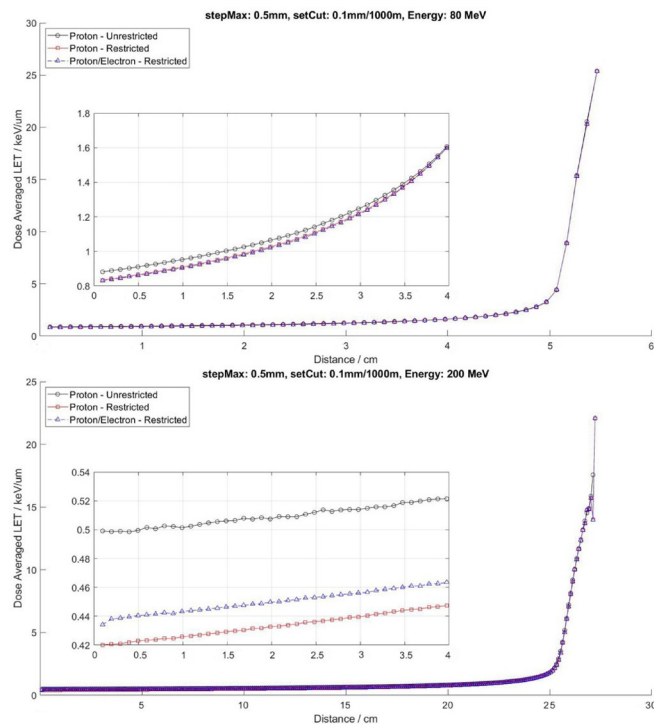
the scoring of LET$_D$. LET$_D$ scoring methods suggested by both Cortes-Giraldo *et al*[20] and Granville *et al*[5] are similar to our *Unrestricted* method.

$$\frac{E\left(\frac{\epsilon_i^2}{l_i}\right)}{E(\epsilon_i)} \approx \frac{\sum_{i=1}^{n_i} \frac{\epsilon_i^2}{l_i}}{\sum_{i=1}^{n_i} \epsilon_i} \times \frac{\frac{1}{n_i}}{\frac{1}{n_i}} \qquad (7)$$

Unrestricted and *Method 1* are similar scoring methods where *Unrestricted* uses high range cut value leading to no secondary electrons production, hence the absence of n_e, ϵ_e and l_e. *Methods 1* and *4* use similar concept to the work by Cortes-Giraldo *et al*[20] method except that energy deposition from secondary electrons were excluded in the calculation. In *Methods 2*, *3* and *4*, energy depositions are summed before dividing by the sum of step length, whereas *Unrestricted* and *Method 1* are summed after each step energy deposition divided by its step length.

In addition, by using **Eq**. (6), we can understand why different scoring methods affect the LET$_D$ results. Thus, Table 1 shows the numerator of each scoring methods expressed in exact mathematical form. Furthermore, by evaluating the reproducibility of LET$_D$ values with different scoring methods at *Positions 1* to *4* (as defined in **Sec**.(2.1)), a set of MC simulation parameters could be recommended.

RESULTS

The results in the variation of LET$_D$ values from different energy cut for 80 MeV and 200 MeV are shown in Figure 2. *Proton–Unrestricted* refers to data from range cut of 1000 m. *Proton–Restricted* and *Proton/Electron–Restricted* refer to data from range cut of 0.01 mm using *Method 1*. The former LET$_D$ calculation factors in only primary proton while the latter accounts for both primary protons and secondary electrons. Figure 2 shows how LET$_D$ values depend on the range cut value set for MC simulation. There is a discrepancy between *Unrestricted* and *Restricted* LET$_D$, especially at the plateau region. This is due to the presence of secondary electrons limited by the range cut. *Unrestricted* LET$_D$ is higher than *Restricted* LET$_D$ despite not including secondary electrons in the calculation. This further proved that we should be careful in choosing the range cut value during simulation.

Correlation analysis

The covariance between energy deposition per step and step length of the proton beam is shown in Figure 3. Individual particle track was scored at selected voxels and the energy deposition per step was plotted for each permutation of energy, step length and range cut. Plots **a**, **b** and **c** represent range cut of 0.01 mm at Position 1; Plots **d**, **e** and **f** represent range cut of 0.05 mm at Position 2; and Plots **g**, **h** and **i** represent range cut of 0.1 mm at Position 3. Plots **a**, **d** and **g** represent step length of 0.01 mm; Plots **b**, **e** and **h** represent step length of 0.05 mm; and Plots **c**, **f** and **i** represent step length of 0.5 mm. Only 200 MeV data was presented as it depicts a similar trend with both 80 MeV and 150 MeV data at *Positions 1, 2* and *3*. Comparing across all simulation parameters, linear and non-linear correlation for both protons and secondary electrons were observed. The *Pearson r-squared* values showed up to 0.99.

Unlike at the plateau region in Figure 3, certain simulation parameters do not show any secondary electrons due to the range cut parameter at the Bragg peak region. Table 3 indicates the presence of secondary electrons in different simulation parameters. Only data from range cut of 0.01 mm at *Position 4* is shown in Figure 4 as secondary electrons are present and it follows a similar trend for other range cut and step length parameters. Plots **a**, **b** and **c** represent step length of 0.01 mm; Plots **d**, **e** and **f** represent step length of 0.05 mm; and Plots **g**, **h** and **i** represent step length of 0.5 mm. Plots **a**, **d** and **g** represent proton beam energy of 80 MeV; Plots **b**, **e** and **h** represent proton beam energy of 150 MeV; and Plots **c**, **f** and **i** represent proton beam energy of 200 MeV.

Table 4 shows the calculated values of the individual terms of **Eq**. (6) at *Position 1*. Data from *Positions 2* and *3* was not shown as it follows similar trend to the data from *Position 1*. The percentage difference accounting for both primary protons and secondary electrons was calculated with respect to $E\left(\frac{\epsilon_i^2}{l}\right)$. It shows that as range cut decreases, the differences between $E\left(\frac{\epsilon_i^2}{l}\right)$ and $\frac{E\left(\epsilon_i^2\right)}{E(l)}$ increase by up to 43%. Results from step length of 0.05 mm show the smallest percentage difference while step length of 0.5 mm shows the largest percentage difference.

Figure 3. This figure shows the plots of energy deposition *vs* step length of both protons and secondary electrons of 200 MeV proton beam at the plateau region. Plots **a**, **b** and **c** represent range cut of 0.01 mm at Position 1; Plots **d**, **e** and **f** represent range cut of 0.05 mm at Position 2; and Plots **g**,**h** and **i** represent range cut of 0.1 mm at Position 3. Plots **a**, **d** and **g** represent step length of 0.01 mm; Plots **b**, **e** and **h** represent step length of 0.05 mm; and Plots **c**, **f** and **i** represent step length of 0.5 mm. The zoomed in plot shows only secondary electrons (red) while the actual plot shows protons (blue) and secondary electrons (red).
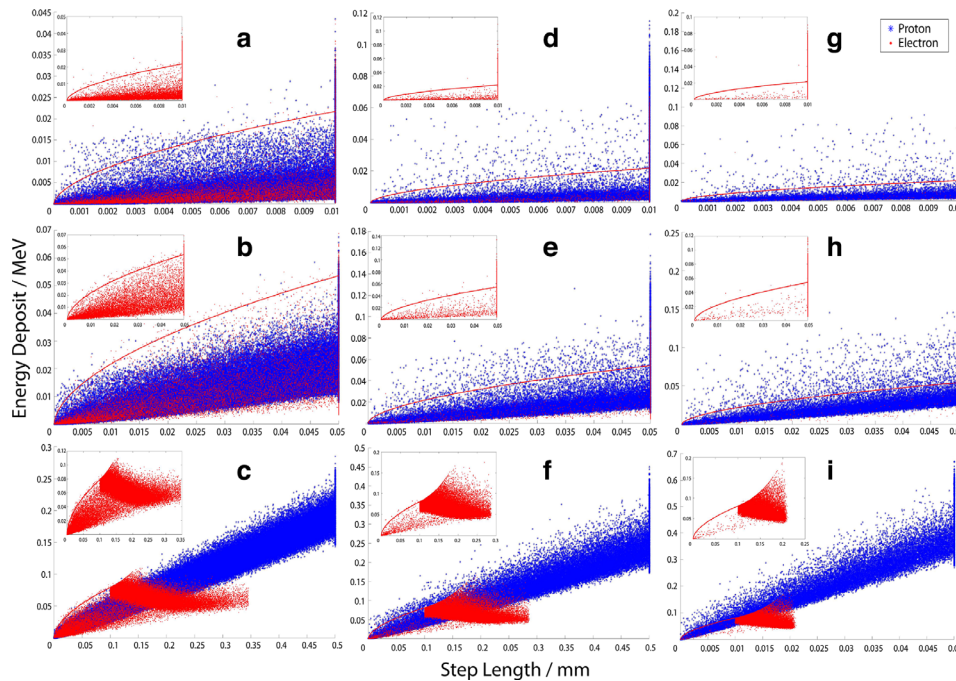
At *Position 4*, the number of secondary electrons decreases as most of the primary protons' energy fall below the cut-off energy. The percentage difference at *Position 1* is much lower (35%) when compared to *Position 1*. *Unrestricted* range cut at all positions gave 0% differences since there is an absence of secondary electrons. We aim to achieve better dose accuracy by accounting for secondary electrons during dose calculation. However, all positions show that as the range cut decreases, the percentage difference between $E\left(\dfrac{\epsilon_i^2}{l}\right)$ and $\dfrac{E\left(\epsilon_i^2\right)}{E(l)}$ increases.

LET_D scoring method analysis

In this section, LET$_D$ values were calculated using five scoring methods at all *Positions* for all permutations of simulation parameters in **Sec**. (2.1). Every *Position* for each *Energy* has three step length values (x-axis) and each step length value would correspond to range cut of 0.01 mm, 0.05 mm and 0.1 mm as represented by (*i*), (*ii*) and (*iii*), respectively in Figure 5. LET$_D$ value determined by *Unrestricted* scoring method is plotted for

all step length. For a 200 MeV proton beam, range cut of 1000 m and step length of 0.5 mm, approximately 1100 protons/second are simulated on single core of an Intel Xeon Gold CPU running at 2.10 GHz. Table 5 shows the CPU time needed for all simulation parameters for 200 MeV and particle histories of 100,000.

Percentage difference between scoring methods was calculated with reference to the *Unrestricted* scoring method LET$_D$ value within each set of simulation protocols. The largest difference of 200% occurs at *Position 3* of 80 MeV, step length of 0.5 mm and range cut of 0.01 mm using *Method 3*. At the Bragg peak region of 200 MeV proton beam, the largest percentage difference (81%) occurs at step length of 0.5 mm and range cut of 0.01 mm using *Method 3*. The percentage difference compared across all energies using *Method 1* is up to 8% regardless of simulation parameters chosen at the Bragg peak region. Furthermore, the percentage difference at Bragg peak region with step length of 0.05 mm and range cut of 0.01 mm is the lowest (up to 45%) as

Table 3. Simulation parameters at *Position* 4. ✔ represents the presence of secondary electrons while ✖ represents the absence of secondary electrons

stepMax	0.5 *mm*			0.05 mm			0.01 *mm*		
setCut	0.01 *mm*	0.05 *mm*	0.1 *mm*	0.01 *mm*	0.05 *mm*	0.1 *mm*	0.01 *mm*	0.05 *mm*	0.1 *mm*
80 MeV	✔	✖	✖	✔	✖	✖	✔	✖	✖
150 MeV	✔	✖	✖	✔	✔	✖	✔	✔	✖
200 MeV	✔	✔	✖	✔	✔	✖	✔	✔	✖

Figure 4. This figure shows the plots of Energy Deposition Vs Step Length of both protons and secondary electrons of 0.01 mm range cut at Position 4. Plots **a**, **b** and **c** represent step length of 0.01 mm; Plots **d**, **e** and **f** represent step length of 0.05 mm; and Plots **g**, **h** and **i** represent step length of 0.5 mm. Plots **a**, **d** and **g** represent proton beam energy of 80 MeV; Plots **b**, **e** and **h** represent proton beam energy of 150 MeV; and Plots **c**, **f** and **i** represent proton beam energy of 200 MeV. The zoomed in plot shows only secondary electrons (red) while the actual plot shows protons (blue) and secondary electrons (red).
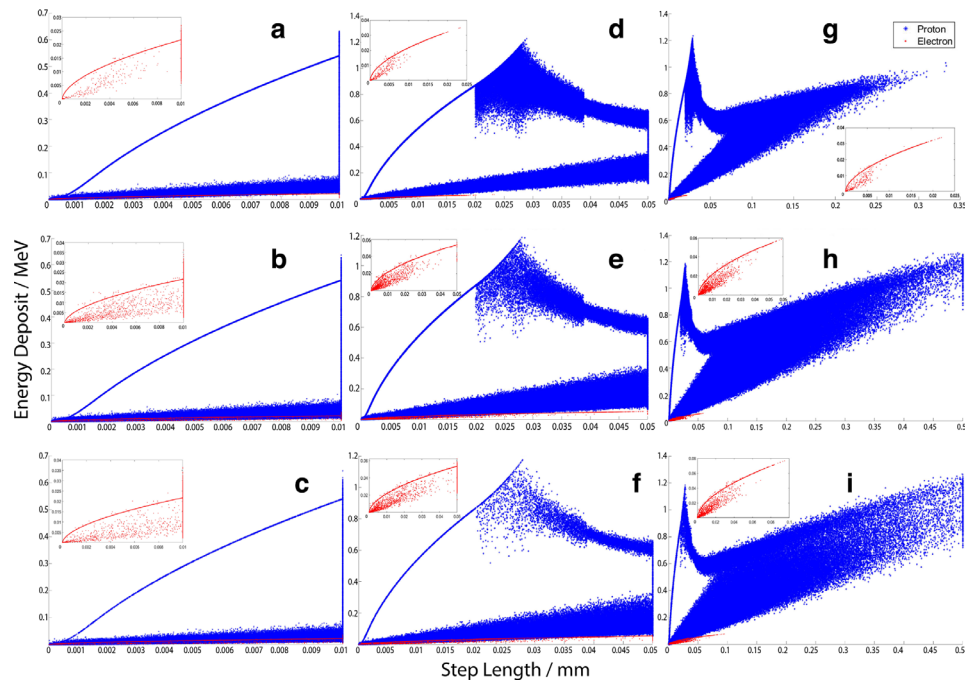
compared to step length of 0.5 mm (up to 81%) and 0.01 mm (up to 47%) with range cut or 0.01 mm. Scoring *Method* 1 has one of the lowest percentage difference compared across all simulation parameters.

DISCUSSION

There had not been a standardized simulation protocol despite the extensive use of MC simulation in proton therapy. Most works adopt their own set of simulation protocols and this is a challenge for the community when comparing LET_D results across institutions.

In this work, we explored the effect of simulation parameters and scoring methods on LET_D. Figure 3 shows data at the plateau region (*Positions 1*, 2 and *3*) for 200 MeV proton beam. Upon closer inspection of the covariance between energy deposition per step and step length of the proton beam, the distribution of the data points explained that $E\left(\frac{\epsilon_i^2}{l}\right)$ could differ slightly with a *r-squared* value of 0.96 (Figure 3 **c**, **f** and **i**) or significantly with a *r-squared* of 9×10^{-5} (Figure 3 **a, b, d, e, g** and **f**) from $\frac{E\left(\epsilon_i^2\right)}{E(l)}$

. This suggests that the choice of scoring methods and simulation parameters should be carefully selected for LET_D calculation since high *r-squared* values relate to higher covariance.

At the Bragg peak region (*Position 4*) in Figure 4, it shows low covariance between energy deposition and step length with the same set of simulation parameters as Figure 3. This implies that

the scoring methods could be arbitrarily selected as the choice of methods will not significantly influence the exact values of LET_D. Therefore, to achieve a reproducible LET_D value, we had calculated and compared the percentage difference between $E\left(\frac{\epsilon_i^2}{l}\right)$ and $\frac{E\left(\epsilon_i^2\right)}{E(l)}$ as shown in Table 4 for each permutation for the simulation parameters. The physical LET_D values were also calculated for each scoring method as shown in Figure 5.

Figure 5 shows that as step length and range cut decrease, the deviation of LET_D values compared among scoring methods increases in all positions. For example, in *Position 1* of 80 MeV, LET_D values among the scoring methods have larger variation for range cut of 0.01 mm as compared to range cut of 0.1 mm. This depicts the same trend for all positions and step length. The percentage difference of LET_D, with respect to *Unrestricted* scoring method, is up to 200% (LET_D values at step length of 0.5 mm and range cut of 0.01 mm at *Position 3* of 80 MeV) depending on which simulation parameters and scoring methods were used. This proves that simulation parameters and scoring methods have to be chosen carefully in MC simulation.

In this work, step length of 0.05 mm is chosen as it shows the most consistency for all range cut and scoring methods throughout all positions. The rest of the step length have their own limitations which will be discussed in the rest of the paragraph. Comparing the percentage difference between $E\left(\frac{\epsilon_i^2}{l}\right)$ and $\frac{E\left(\epsilon_i^2\right)}{E(l)}$ throughout the Bragg peak curve, step length of 0.5 mm is not recommended

Table 4. Percentage difference at *Position 1* (Plateau region) between $E\left(\frac{\epsilon^2}{l}\right)$ and $\frac{E\left(\epsilon_i^2\right)}{E(l_i)}$ given by the second and third terms of **Eq.**4, using $E\left(\frac{\epsilon^2}{l}\right)$ as reference

Energy	stepMax setCut	0.5 mm $E\left(\frac{\epsilon^2}{l}\right)$	$\frac{E\left(\epsilon_i^2\right)}{E(l_i)}$	$-\frac{Cov\left(\epsilon_i^2,l\right)}{(E(l))^2}+\frac{Var(l)\,E\left(\epsilon_i^2\right)}{(E(l))^3}$	% Difference	0.05 mm $E\left(\frac{\epsilon^2}{l}\right)$	$\frac{E\left(\epsilon_i^2\right)}{E(l_i)}$	$-\frac{Cov\left(\epsilon_i^2,l\right)}{(E(l))^2}+\frac{Var(l)\,E\left(\epsilon_i^2\right)}{(E(l))^3}$	% Difference	0.01 mm $E\left(\frac{\epsilon^2}{l}\right)$	$\frac{E\left(\epsilon_i^2\right)}{E(l_i)}$	$-\frac{Cov\left(\epsilon_i^2,l\right)}{(E(l))^2}+\frac{Var(l)\,E\left(\epsilon_i^2\right)}{(E(l))^3}$	% Difference
80 MeV	10 µm	0.084	0.171	-0.123	42.423	0.029	0.029	1.09E-04	0.075	0.008	0.007	1.89E-04	2.303
	50 µm	0.223	0.309	-0.036	22.152	0.037	0.037	-1.16E-05	0.463	0.010	0.010	2.75E-05	0.389
	100 µm	0.274	0.344	-0.022	17.056	0.040	0.040	-1.28E-05	0.253	0.012	0.012	1.31E-05	0.153
150 MeV	10 µm	0.053	0.079	-0.028	3.429	0.014	0.012	5.64E-04	8.118	0.004	0.003	1.45E-04	4.437
	50 µm	0.095	0.118	-0.010	13.153	0.015	0.015	1.05E-04	0.877	0.005	0.005	2.57E-05	0.864
	100 µm	0.108	0.128	-0.008	11.464	0.016	0.016	6.02E-05	0.443	0.006	0.005	1.44E-05	0.412
200 MeV	10 µm	0.044	0.057	-0.014	2.663	0.011	0.009	5.43E-04	11.077	0.003	0.003	1.19E-04	5.006
	50 µm	0.069	0.081	-0.006	8.856	0.011	0.011	1.07E-04	1.463	0.004	0.003	2.18E-05	1.020
	100 µm	0.076	0.087	-0.005	8.182	0.012	0.012	6.435E-05	0.755	0.004	0.004	1.299E-05	0.500

due to its highest percentage difference. In addition, the differences of LET_D values compared among different scoring methods could differ up to 200%. With step length of 0.01 mm, Figure 5 shows an initial decrease at the plateau region before increasing towards the Bragg peak and this is physically incorrect due to small step size artefacts[4]. Thus, it is not recommended due to the large variance from different scoring methods. Therefore, 0.05 mm is the recommendation for step length to be used in MC simulation.

Subsequently, a range cut of 0.01 mm is chosen since the priority is to obtain a better dose accuracy by including explicit electron transports in the medium. When a high range cut is chosen, there will be fewer or an absence of secondary electrons at the Bragg peak region. Thus, LET_D scoring methods as shown in Table 1 would converge to Table 6. *Method 1* would be the same as *Unrestricted* while *Methods 2* and *3* are equal.

We expect the percentage difference arising from different LET_D scoring methods to decrease as it approaches the Bragg peak. This is explained by the low covariance (Figure 4) and the convergence of scoring methods (Table 6) at the Bragg peak region. However, at low energy with a range cut of 0.1 mm or 0.05 mm, the percentage difference decreases along the plateau and increases as it approaches the Bragg peak. The percentage difference is up to 65% (plateau region) and 41% (Bragg peak region) for these range cut (0.1 mm and 0.05 mm). Despite having larger percentage difference of up to 72% (plateau region) and 59% (Bragg peak region) with range cut of 0.01 mm at 200 MeV, it shows the greatest consistency throughout all energies. Thus, step length of 0.05 mm and range cut of 0.01 mm is a suitable set of simulation parameters for proton therapy.

Pertaining to LET_D scoring methods, we could observe that LET_D values calculated from *Method 3* deviate from other scoring methods at step length of 0.05 mm and range cut of 0.01 mm along the plateau region (*Positions 1*, 2 and *3*) in Figure 5. It is expected at the Bragg peak region (*Position 4*) that LET_D values calculated using *Method 2* will be similar to using *Method 3* and this is analogous to *Method* 1 and *Unrestricted* due to the decrease of secondary electrons at *Position 4*. LET_D values calculated using *Method 4* deviate from other scoring methods at *Position 4*. Therefore, it is more appropriate to use *Method 1* since the LET_D values are approximately the average of other scoring methods.

From what we have discussed above, we recommend a set of simulation parameters and scoring method that would result in a most reproducible LET_D. We recommend using step length of 0.05 mm and range cut of 0.01 mm for all range of energies and scoring *Method 1* for LET_D calculation. This method can be generalized for a clinically relevant Spread-Out Bragg Peak (SOBP) by introducing a weighting factor to Table 1. The expectation form of each methods will need to include the weighted sum of the individual expectation for mono-energetic proton beam as shown in **Eq.** (8). The weight (w_j corresponds to the relative contribution of each mono-energetic proton (denoted by j) required to make up the SOBP.

Figure 5. This figure shows the LET$_D$ values calculated using each scoring methods as represented by different symbols for all simulation parameters at Positions 1, 2, 3 and 4. Range cut of 0.01 mm, 0.05 mm and 0.1 mm is represented by (i), (ii) and (iii), respectively, and it is similar for all subsequent step length. Positions 1, 2 and 3 share the same y-axis while Position 4 uses its own y-axis due to higher LET$_D$ values at the Bragg peak region.

$$\sum_{j=1}^{n} w_j \frac{\mathrm{E}\left(\frac{\epsilon_i^2}{l_i}\right)}{\mathrm{E}(\epsilon_i)}$$
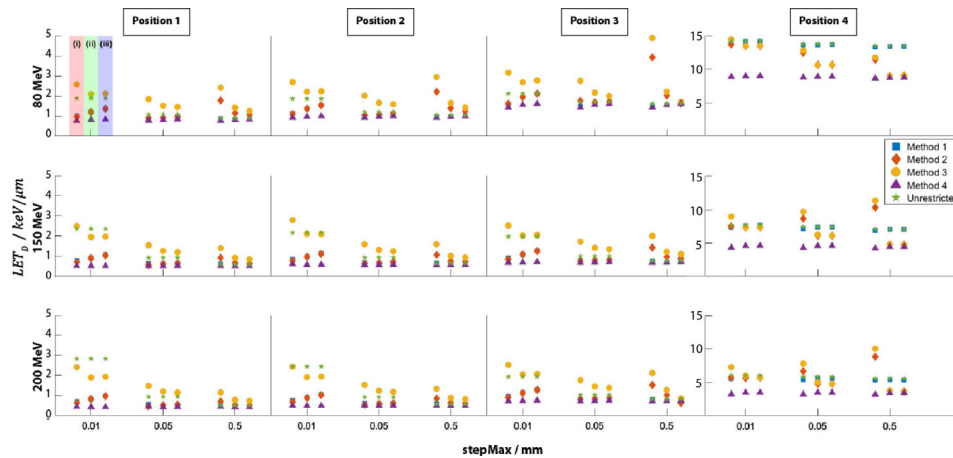
Furthermore, this recommendation can be applied for other ions which are used clinically such as Carbon or Helium despite being a challenge when tracking the large number of secondary electrons

Table 5. CPU time (in protons/second) used for 200 MeV proton beam with different range cut and step size using 10,0000 particles

200 MeV	Range Cut			
Step length	0.01 mm	0.05 mm	0.1 mm	1000 m
0.01 mm	20	22	23	25
0.05 mm	83	106	111	120
0.5 mm	200	666	714	1111

and the inclusion of huge species of nuclear secondary products. This recommendation would allow us to consider for better dose calculation accuracy and LET$_D$ consistency in future simulation results.

CONCLUSION

Our study shows that the simulation parameters and LET$_D$ scoring methods are important when they come to obtain a reproducible LET$_D$ value MC method. This had prompted us to investigate how the simulation parameters and scoring methods affect our LET$_D$ results. Overall, we recommend step length of 0.05 mm, range cut of 0.01 mm and scoring *Method 1* for LET$_D$ calculation to be used in MC simulation so as to obtain a more reproducible LET$_D$ values. By establishing these MC simulation protocols, we hope that this would benefit future work in obtaining a more precise biological dose calculation by including a more standardized LET$_D$ values in the RBE formula.

Table 6. *LET$_D$* Scoring methods when there is an absence of secondary electrons

Unrestricted	Method 1	Method 2	Method 3	Method 4
$\dfrac{\sum_{p=1}^{n_p} \frac{\epsilon_p^2}{l_p}}{\sum_{p=1}^{n_p} \epsilon_p}$	$\dfrac{\sum_{p=1}^{n_p} \frac{\epsilon_p^2}{l_p}}{\sum_{p=1}^{n_p} \epsilon_p}$	$\dfrac{\frac{\sum_{p=1}^{n_p} \epsilon_p^2}{\sum_{p=1}^{n_p} l_p}}{\frac{\sum_{p=1}^{n_p} \epsilon_p}{n_p}}$	$\dfrac{\frac{\sum_{p=1}^{n_p} \epsilon_p^2}{\sum_{p=1}^{n_p} l_p}}{\frac{\sum_{p=1}^{n_p} \epsilon_p}{n_p}}$	$\dfrac{\frac{\left(\sum_{p=1}^{n_p} \epsilon_p\right)^2}{\sum_{p=1}^{n_p} l_p}}{\sum_{p=1}^{n_p} \epsilon_p}$

REFERENCES

1. McMahon SJ, Paganetti H, Prise KM. LET-weighted doses effectively reduce biological variability in proton radiotherapy planning. *Phys Med Biol* . 2018; **63**: 225009Available from[Internet]. doi: https://doi.org/10.1088/1361-6560/aae8a5

2. Paganetti H. Relative biological effectiveness (RBE) values for proton beam therapy. variations as a function of biological endpoint, dose, and linear energy transfer. *Phys Med Biol* 2014; **59**: R419–72. doi: https://doi.org/10.1088/0031-9155/59/22/R419

3. Wilkens JJ, Oelfke U. A phenomenological model for the relative biological effectiveness in therapeutic proton beams. *Phys Med Biol* 2004; **49**: 2811–25. doi: https://doi.org/10.1088/0031-9155/49/13/004

4. Guan F, Peeler C, Bronk L, Geng C, Taleei R, Randeniya S, et al. Analysis of the track- and

dose-averaged let and let spectra in proton therapy using the geant4 Monte Carlo code. *Med Phys* . 2015; **42**: 6234–47Available from[Internet]. doi: https://doi.org/10.1118/1.4932217

5. Granville DA, Sawakuchi GO. Comparison of linear energy transfer scoring techniques in Monte Carlo simulations of proton beams. *Phys Med Biol* 2015; **60**: N283–91. doi: https://doi.org/10.1088/0031-9155/60/14/N283

6. Wilkens JJ, Oelfke U. Analytical linear energy transfer calculations for proton therapy. *Med Phys* 2003; **30**: 806–15. doi: https://doi.org/10.1118/1.1567852

7. Grassberger C, Paganetti H. Elevated let components in clinical proton beams. *Phys Med Biol* 2011; **56**: 6677–91. doi: https://doi.org/10.1088/0031-9155/56/20/011

8. Romano F, Cirrone GAP, Cuttone G, Rosa FD, Mazzaglia SE, Petrovic I, et al. A Monte Carlo study for the calculation of the average linear energy transfer (let) distributions for a clinical proton beam line and a radiobiological carbon ion beam line. *Phys Med Biol* 2014; **59**: 2863–82. doi: https://doi.org/10.1088/0031-9155/59/12/2863

9. Seco J, Verhaegen F. Monte Carlo techniques in radiation therapy. Vol. 42, medical physics. *CRC/Taylor & Francis* 2013;: 342p..

10. Ray S, Cekanaviciute E, Lima IP, Sørensen BS, Costes SV. Comparing photon and charged particle therapy using DNA damage biomarkers. *Int J Part Ther* 2018; **5**: 15–24.

doi: https://doi.org/10.14338/IJPT-18-00018.1

11. Wang W, Li C, Qiu R, Chen Y, Wu Z, Zhang H. Modelling of cellular survival following radiation-induced DNA double-strand breaks. *Sci Rep* . 2018;: 1–12Available from[Internet].

12. Qi Tan H, Yang Calvin Koh W, Kuan Rui Tan L, Hao Phua J, Wei Ang K, Yong Park S, Tan HQ, Koh, Wei Yang C, LKR T, Phua JH, Ang KW, et al. Dependence of let on material and its impact on current RBE model. *Phys Med Biol* 2019; **64**: 135022. doi: https://doi.org/10.1088/1361-6560/ab1c90

13. Cortés-Giraldo MA, Carabe A. A critical study of different Monte Carlo scoring methods of dose average linear-energy-transfer maps calculated in voxelized geometries irradiated with clinical proton beams. *Phys Med Biol* 2015; **60**: 2645–69. doi: https://doi.org/10.1088/0031-9155/60/7/2645

14. Seltzer SM. ICRU Report 85 FUNDAMENTAL QUANTITIES AND UNITS FOR IONIZING RADIATION.. 201111(1). Available from:Jicru [Internet].. Available from: http://jicru.oxfordjournals.org/.

15. Fippel M, Soukup M. A Monte Carlo dose calculation algorithm for proton therapy. *Med Phys* 2004; **31**: 2263–73. doi: https://doi.org/10.1118/1.1769631

16. Schümann J, Paganetti H, Shin J, Faddegon B, Perl J. Efficient voxel navigation for proton therapy dose calculation in TOPAS and

Geant4. *Phys Med Biol* 2012; **57**: 3281–93. doi: https://doi.org/10.1088/0031-9155/57/11/3281

17. Allison J. Geant4–a simulation toolkit. *Int J Phytoremediation* 2007; **17**: 20–4.

18. Yoshida H, Cuttone G, Sasaki T, Pfeiffer A, Truscott P, Larsson S, et al. Geant4 developments and applications. *IEEE Trans Nucl Sci* 2006; **53**: 270–8.

19. Allison J, Amako K, Apostolakis J, Arce P, Asai M, Aso T, et al. Recent developments in Geant4. *Nuclear Instruments and Methods in Physics Research Section A: Accelerators, Spectrometers, Detectors and Associated Equipment* 2016; **835**: 186–225. doi: https://doi.org/10.1016/j.nima.2016.06.125

20. Cortés-Giraldo MA, Carabe A. A critical study of different Monte Carlo scoring methods of dose average linear-energy-transfer maps calculated in voxelized geometries irradiated with clinical proton beams. *Phys Med Biol* 2015; **60**: 2645–69. doi: https://doi.org/10.1088/0031-9155/60/7/2645

21. Elandt-Johnson RC, Johnson NL. *Survival models and data analysis*. New York : Wiley; 198069 p..

22. Kendall MG, Stuart A, Ord JK, Arnold SF, O'Hagan A. *Kendall's Advanced Theory of Statistics*. 6th Editio. London : Edward Arnold ; New York : : Halsted Press; 1998351 p.